Received: 28 March 2022 | Revised: 18 September 2022 | Accepted: 26 October 2022

DOI: 10.1002/kin.21620

INTERNATIONAL JOURNAL OF CHEMICAL KINETICS WILEY

RESEARCH ARTICLE

Kinetic adsorption of drugs using carbon nanofibers in simulated gastric and intestinal fluids

Elif Caliskan Salihi | **Betül Berber** | **Kübra İsanç**

Faculty of Pharmacy, Department of Basic Pharmaceutical Sciences, Marmara University, Istanbul, Turkey

Correspondence
Elif Caliskan Salihi, Marmara University, Faculty of Pharmacy, Department of Basic Pharmaceutical Sciences, 34854 Istanbul, Turkey.
Email: caliskanelif@gmail.com

Abstract

Two different classes of drugs were selected to test the adsorption capacity of carbon nanofibers as a greener new generation alternative adsorbent in simulated gastric and intestinal fluids. Kinetics of the promethazine and trimethoprim adsorption were analyzed using Lagergren first order and Pseudo second order models. Intraparticle diffusion graphs were also plotted to discuss the adsorption mechanism. Kinetic data showed the significance of boundary layer effect for both of the drugs and the presence of intraparticle diffusion as the other rate controlling step for the promethazine adsorption. Giles isotherms showed the high affinity of drug molecules to the adsorbent. Maximum adsorption capacity of drugs was calculated using Langmuir model as 18.35 and 41.15 mg/g for trimethoprim and 95.24 and 80.65 mg/g for promethazine in simulated gastric fluid (SGF) and simulated intestinal fluid (SIF), respectively. Trimethoprim adsorption was under favor of hydrophobic interaction and π-π dispersion interactions while promethazine adsorption was through cation exchange where the electrostatic attraction is an important force with the contribution of dispersion interactions.

KEYWORDS
adsorption, carbon nanofibers, kinetics, promethazine, trimethoprim

1 | INTRODUCTION

Xenobiotic exposure knowingly or accidentally is a real risk which can lead to fatal poisoning. Poisoning owing to drug overdose is one of the leading emergent cases among the hospital admissions.[1] Many drugs in use do not have specific antidotes for the treatment. It is essential to prevent the further absorption of drug if the antidote is unavailable. Gastrointestinal adsorbents such as activated carbon play the key role for the decontamination of toxic effects of the xenobiotics from the body.[2] However, there is only a number of studies on the adsorption kinetics and capacity of a specific adsorbent for known drugs in simulated gastric and intestinal fluids and there is no study on the adsorption performance of CNF in simulated gastric and intestinal fluids. Previous adsorption studies carried by using simulated gastric and intestinal medium were summarized below.

Sah et al. have investigated in vitro diazepam adsorption by activated charcoal and the effect of pH besides the presence of ethanol using simulated gastric and intestinal fluids. They have reported that activated charcoal has the capacity to adsorb sufficient amounts of diazepam belongs to benzodiazepines class which is among the major drug types responsible for self-poisoning in the world.[3] Stefan et al. have studied the influence of internal structure of the adsorbents on diazepam adsorption in simulated intestinal fluid (SIF) and reported the higher adsorption capacity of activated carbon than mineral clay since the activated carbon has a pore volume which is much higher than the one of the mineral clay. Another important result is the uptake of diazepam by both adsorbents decreases

in the presence of ethanol.[4] Regmi et al. have reported in vitro adsorption of dextromethorphan syrup which is an over-the-counter antitussive drug using activated charcoal in simulated gastric and intestinal fluids. They have showed that the use of activated charcoal might be the most effective approach for the dextromethorphan overdose treatment.[5] Nabais et al. have tested one of the most widely used antidepressant drugs, fluoxetine removal capacity of activated carbons, and activated carbon fibers.[6] Commercial activated carbon was also tested for metamizole sodium (dipyrone) adsorption in simulated gastric and intestinal fluids at the temperature of human body in one of our previous studies. Results showed the fast and effective adsorption of activated carbon for the metamizole sodium which usually causes mild toxicity in the case of overdose which occurs mainly at home by the oral route in relation to a considerable number of suicide attempts.[7] Wang et al. have prepared and used processed montmorillonite clays for the adsorption of polychlorinated biphenyls which have been detected as prevalent environmental contaminants in water, food and biota.[8] Wang et al. have used zwitterionic montmorillonites for the simultaneous detoxification of aflatoxin B1 and zearalenone from simulated gastrointestinal tract and demonstrated the ability of zwitterionic montmorillonites for the detoxification of mycotoxins with different polarities.[9] Rasheed et al. modified the bentonite clay using orange peels extract and used as mycotoxins' binder in simulated gastrointestinal fluids and reported the adsorption capacity for the mycotoxins after modification.[10] There are also few studies that reported the development of enterosorbents for toxin adsorption.[11–13]

Concordantly, this study was designed to test the adsorption capacity and to understand the adsorption mechanism of carbon nanofibers (CNF) for selected drugs in simulated gastric fluids (SGF) and SIF. Promethazine (PM) and trimethoprim (TMP) were selected as model drugs from different classes. PM is a phenothiazine derivative acts as an antihistamine and used to treat allergy, nausea and sleep difficulty. PM may also be used for sedation for anxiety. It is a frequently used drug and overdose cases were reported related to suicide attempts during pregnancy.[14] TMP belongs to antibiotic class and is used primarily for urinary tract infections besides any susceptible aerobic bacterial species. It is used for the treatment of various bacterial infections in combination with sulfamethoxazole (TMP/SMX) as co-trimoxazole. However, it is necessary to recognize the potential of TMP to cause anaphylaxis which is a severe, systemic allergic reaction carrying a high mortality risk.[15]

Commercial CNF which was supplied as a greener advanced material alternative in its raw form was used as adsorbent for PM and TMP removal in SGF and SIF. CNF is a nanosized fiber form material with a hollow core and sp^2-based atomic order as subsequent graphene layers. CNF has a potential for a wide range of applications from pharmaceutical industry to high technology electronics for being flexible, conductive and porous. It is a candidate to be new generation green material of future for bioapplications.[16–20] Adsorption capacity and types of the interactions of CNF surface with drug molecules were revealed in this study. Results of the current study showed the feasibility of CNF to be used in the conditions of SGF and SIF.

2 | MATERIALS AND METHODS

2.1 | Materials and characterization

PM hydrochloride (purity >98%) and TMP (purity ≥98%) were obtained from Sigma and used as received. Molecular structure and properties of drugs were given in Table 1. CNF has a conical shape and was obtained from Sigma-Aldrich (Merck, 719811) as a greener alternative commercial product and was used in powder form. Characterization data of CNF was obtained from the supplier and approved before the adsorption studies. Properties and characterization of CNF were reported in elsewhere.[20] Briefly, CNF used is pyrolitically stripped and comprised of conical platelets. The structure of CNF is carbon basis (>98%) with an average diameter of 130 nm. Average pore volume of CNF is 0.12 cm^3/g and average pore diameter is 89.3 Å. CNF has an average specific surface area of 54 m^2/g with a PHPZC value of 4.9.[20] CNF was washed using distilled water to clean the impurities and dried in the oven at 100°C for 1 day. Total 1 L of distilled water was used for washing 10 g of CNF with the help of a magnetic stirrer. Morphology of CNF was scanned with SEM (Scanning Electron Microscope).

2.2 | Adsorption experiments

Batch adsorption process was conducted using CNF as adsorbent and selected drug molecules (PM and TFP) as adsorbates seperately. Batch adsorption process depends on the contact of adsorbent material with adsorbate solutions with known concentrations during known time intervals. Shaking and fixed temperature were applied during the adsorption process. Calculations were done depending on the differences of the concentrations of the adsorbate solutions before and after the adsorption. The details of the experimental arrangements were given below. Adsorption experiments were done in SGF and SIF at 37°C which is the temperature of human body. Stock

TABLE 1 Molecular structure and properties of drugs

	Molecular structure	Molecular weight (g/mol)	pKa	Water solubility
PM	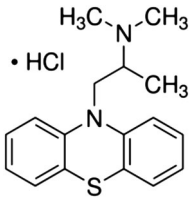	320.88	9.1[a]	Very soluble[b]
TMP	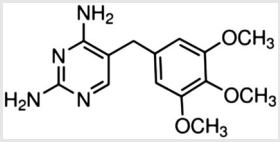	290.32	7.3[c]	400 mg/L[d]

a[21]
b[22]
c[23]
d[24]

solutions of PM and TFP were prepared in SGF (pH = 1.2) which contains NaCl and concentrated HCl (pepsin omitted) and SIF (pH = 7.5) which contains NaH_2PO_4 and NaOH (without pancreatin). Adsorbent/adsorbate ratio was found by conducting preliminary studies and the same ratio was used for all adsorption experiments. Time to reach equilibrium was studied using 0.005/0.01 g CNF and 25 mL of drug solutions (50 mg/L). Samples were taken during and after the adsorption at predetermined intervals followed by filtering. Absorbances of the sample solutions were measured by using a UV-Visible spectrophotometer (Shimadzu). Thereafter, 25 mL of drug solutions with a known concentration between 5 and 50 mg/L were shaken with 0.01 g CNF in 100 mL light-tight glass erlenmeyer flasks at 37°C during the equilibrium time (1 h for PM and 30 min for TMP) using a thermostatic shaker with a water bath. Samples were seperated from CNF with 0.45 μm microfilters. Concentrations of the drug solution samples were measured using spectrophotometer at 302 nm for PM and 278 nm for TMP. Calibration curves prepared initially were used to calculate the concentrations of the samples. Effect of the pH study was done by using drug solutions prepared at various pHs between 1.2 and 11 using the same experimental arrangement. Blank tests were done without the adsorbent. All experiment series were conducted at least three times under identical conditions. The amount of adsorption (q, mg/g) was found with the Equation (1) below:

$$q = \frac{(C_0 - C)V}{w} \quad (1)$$

C_0 (mg/L) shows the concentration of the sample solutions before the adsorption, C (mg/L) shows the concentration of the sample solutions after the adsorption, V shows the volume which is 25 mL and w is the mass of CNF which is 0.01 g. % Adsorption was calculated using the Equation (2) below:

$$Adsorption\% = \frac{(C_0 - C)}{C_0} \times 100\% \quad (2)$$

3 | RESULTS AND DISCUSSION

Decontamination capacity of conical shaped carbon based nanofibers (CNF) was evaluated using PM and TMP in simulated gastric and intestinal fluids (SGF and SIF). Electron microscopy is used to characterize the structure of the materials at the small scale. SEM images were recorded to see the morphology and dimensions of the fibers and given in Figure 1. Nanoscale fibrous structure of the material is seen in both SEM images.

In vitro adsorption experiments were conducted at 37°C using constant amounts of CNF in SGF and SIF. Influence of shaking time on the capacity of adsorption was worked to determine the time to reach equilibrium. Influence of time on the PM adsorption was shown in Figure 2A and equilibrium time was found to be 1 h as seen from the figure. Although the equilibrium time is 1 h, it is seen that more than 50% of the whole adsorption capacity was achieved in 5 min when the adsorbent dose increased to 10 mg (Figure 2B) in this process. Equilibrium time for TMP was found to be 30 min (Figure 3A) but an important amount of the adsorption occured in the first 5 min (Figure 3B) similarly to the PM adsorption. Results showed the fast adsorption of both drugs on CNF and the time to reach equilibrium was not changed with pH of the media.

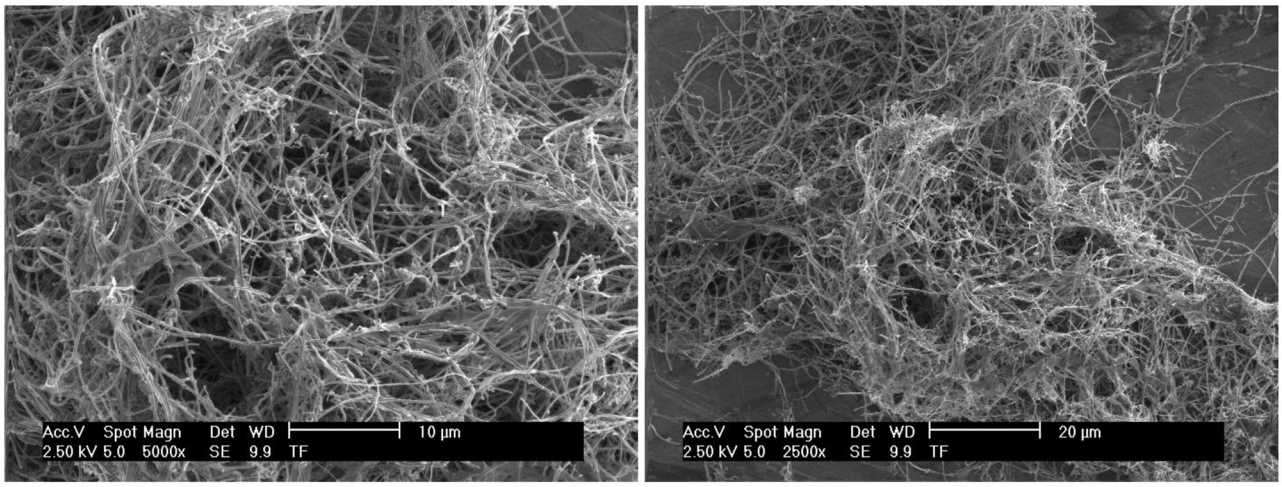

FIGURE 1 SEM images of carbon nanofibers (CNF).

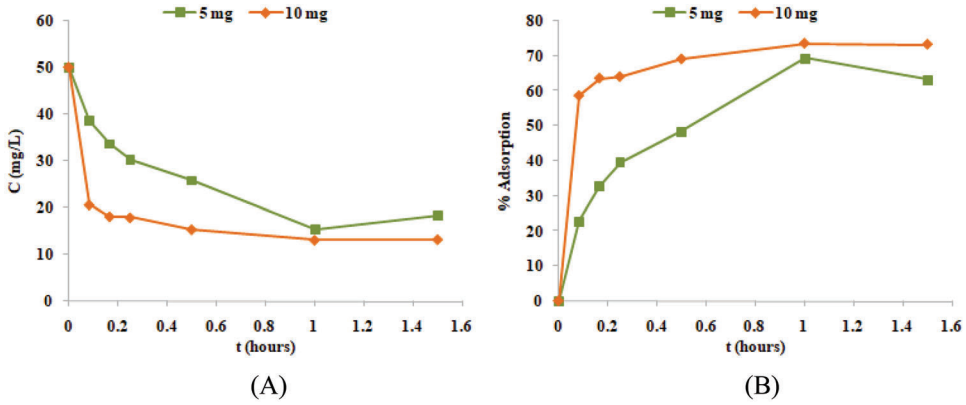

FIGURE 2 Effect of time on the (A) PM concentration; (B) % Adsorption of PM adsorption on CNF.

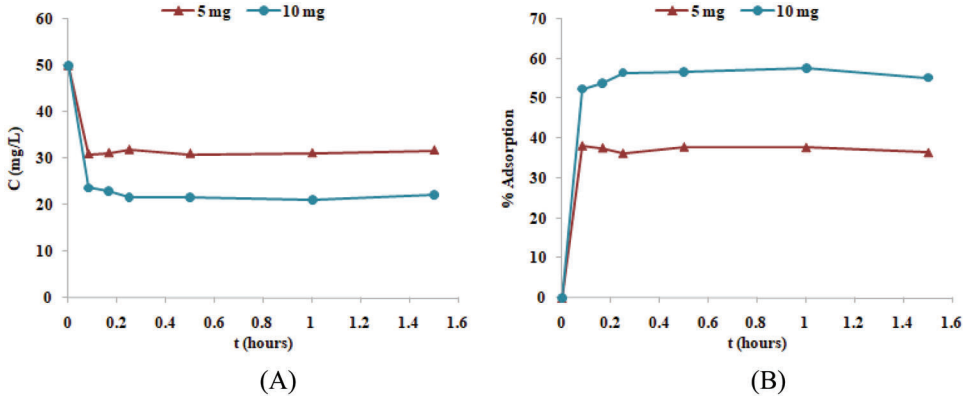

FIGURE 3 Effect of time on the (A) TMP concentration; (B) % Adsorption of TMP adsorption on CNF.

Lagergren first order and Pseudo second order equations were used to model the kinetics of adsorption. Intra-particle diffusion model was applied to understand the adsorption mechanism. Kinetic models were used to calculate the parameters given in Table 2. q_e shows the quantity of adsorption at equilibrium; q is the quantity of adsorption at any time t; and k_1, k_2, k_d are the kinetic constants. Adsorption of the both drugs was suited to Pseudo

TABLE 2 Adsorption kinetics data for drug adsorption on CNF

		Lagergren first order model $ln(q_e - q) = lnq_e - k_1 t$			Pseudo second order model $\frac{t}{q} = \frac{1}{k_2 q_e^2} + \frac{1}{q_e} t$			Intraparticle diffusion $q = k_d t^{1/2}$	
	CNF	k_1 (h^{-1})	q_e (mg/g)	R^2	k_2 (g/mg h)	q_e (mg/g)	R^2	k_d	R^2
PM	5 mg	2.27	73.63	0.924	2.52×10^{-7}	93.46	0.984	75.22	0.982
	10 mg	4.69	43.42	0.748	4.49×10^{-8}	94.34	1.000	25.11	0.966
TMP	5 mg	12.67	11.52	0.406	7.16×10^{-8}	45.77	0.999	-	-
	10 mg	21.38	58.97	0.939	4.08×10^{-9}	69.98	0.999	-	-

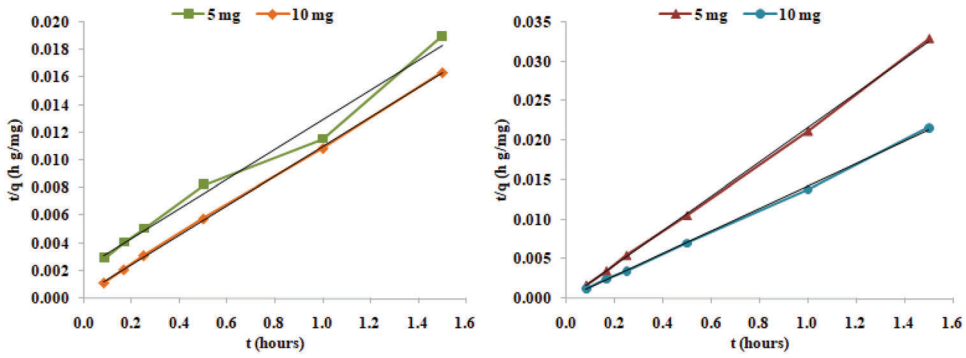

FIGURE 4 Kinetic plots of Pseudo second order model for the PM and TMP adsorption on CNF.

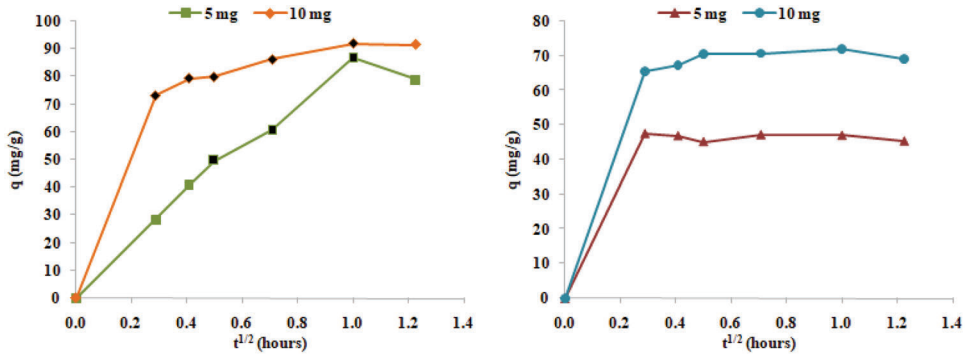

FIGURE 5 Intraparticle diffusion lots for the PM and TMP adsorption on CNF.

second order model (see Figure 4 for the graphs). Intraparticle diffusion graphs were given in Figure 5. Intraparticle diffusion constant (k_D) was calculated for PM adsorption using this linear part of the graph. Plots show the presence of intraparticle diffusion step for the adsorption of PM on CNF (Figure 5A). Linear parts do not cross the origin of the plot showing that there is one more step other than intraparticle diffusion to control the rate of this adsorption process. Figure 5B shows the intraparticle diffusion model for TMP adsorption. On the contrary, intraparticle diffusion was not observed for TMP. The step that controlling the TMP adsorption rate is the diffusion through boundary layer.[25,26]

Total 0.01 g CNF and 25 mL of drug solutions (5–50 mg/L) were used to conduct the equilibrium experiments at 37°C in SGF and SIF during 1 h which is equilibrium time for PM and 30 min for TMP. Equilibrium data were used to plot the Giles isotherms (Figure 6). q shows the adsorption quantity at equilibrium in mg/g. Giles isotherms of PM and TMP adsorption are all H-type considering to Giles classification. H-type of the Giles isotherm shows high affinity between CNF and drugs and it is a special type of L-type Giles isotherm. Both PM and TFP molecules showed high affinity to the surface of the adsorbent.[27,28]

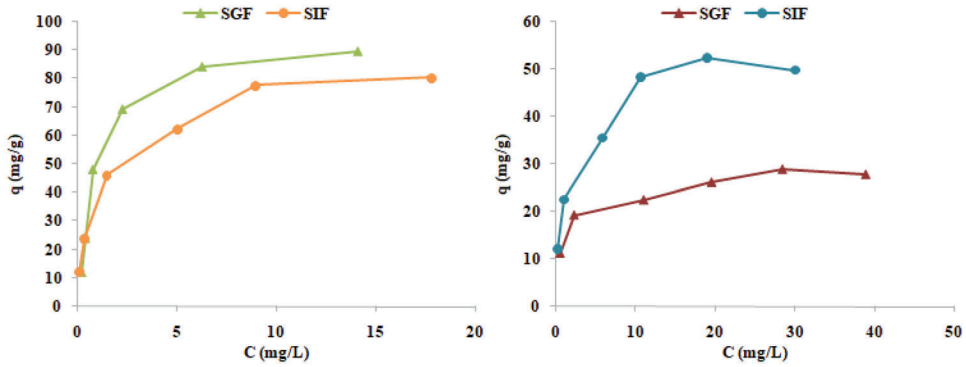

FIGURE 6 Giles isotherms of the PM and TMP adsorption on CNF in SGF and SIF.

TABLE 3 Model fitting of the isotherms of the adsorption of PM and TMP on CNF

		Langmuir model $\frac{C}{q} = \frac{1}{Qb} + \frac{C}{Q}$			Freundlich model $lnq = lnk + n\,lnC$		
		Q (mg/g)	b (L/g)	R^2	k	n	R^2
TMP	SGF	18.35	1.59	0.995	14.09	0.21	0.942
	SIF	41.15	1.29	0.993	21.43	0.29	0.974
PM	SGF	95.24	1.02	0.999	37.10	0.44	0.858
	SIF	80.65	1.05	0.996	33.25	0.37	0.970

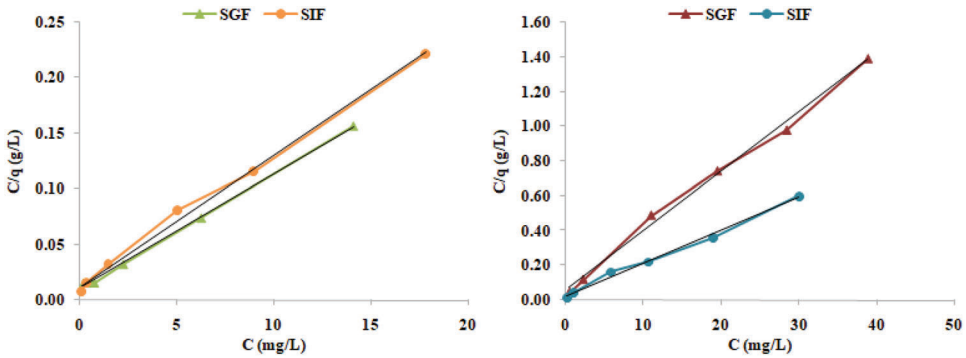

FIGURE 7 Langmuir isotherms of the PM and TMP adsorption on CNF in SGF and SIF.

Equilibrium data of the PM and TMP adsorption was modeled using the isotherm equations and the constants of the isotherms were given in Table 3. Langmuir model (Figure 7) fitted better to the adsorption processes of both of the drugs in SGF and SIF. The Langmuir model shows a monolayer coverage during the localized adsorption and that the molecules of the adsorbates do not locate vertically where they do not compete with the solvent molecules strongly[29,30] Q is the Langmuir equation constant and shows the maximum adsorption capacity. Adsorption capacity of CNF for TMP in SGF was found to be 18.35 mg/g and the capacity was increased to 41.15 mg/g in SIF. Adsorption capacity was found to be higher in the case of PM which is 95.24 mg/g in SGF and 80.65 mg/g in SIF. As a comparison, adsorption capacity of activated carbon for metamizole sodium was found to be 185.19 and 161.29 mg/g in SGF and SIF, respectively. The adsorption capacity increased with decreasing pH in this previous study where electrostatic interactions were the driving force with a possible contribution of π-π dispersion interactions.[7] The results found in this current study showed the potential of CNF in order to be used as a greener alternative advanced material.

According to the results, maximum adsorption capacity for TMP in SIF was found to be much higher than the one in SGF. On the other hand, maximum adsorption capacity for PM in SGF was found to be partially higher than the one in SIF. Effect of pH on the adsorption capacity is

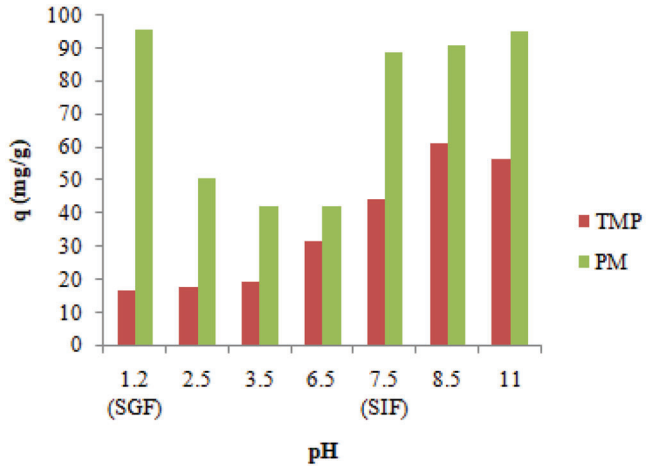

FIGURE 8 Influence of solution pH on the adsorption of drugs on CNF.

an important parameter to disclose the possible interactions between drug molecules and CNF surface taking into account the altering surface charges of CNF and speciation of the drug molecules in the solution depending on the pH. Influence of the pH of the adsorption medium was investigated to further understand the mechanism of the adsorption processes (Figure 8). Experiments were conducted at various pHs between 1.2 and 11. TMP adsorption on CNF was increased importantly with the increase in the pH. pKa of TMP is 7.3 as given in Table 1. TMP molecules present in the solution as cationic species at the pHs lower than 7.3 and neutral species at the pHs higher than 7.3. In addition to this, pH_{PZC} of CNF is 4.9 showing the surface of CNF is positively charged at the pHs lower than 4.9 and negatively charged at the pHs higher than 4.9. So, the adsorption of cationic TMP molecules onto the cationic CNF surface can be explained by hydrophobic interaction and π-π dispersion interactions. Because there is an electrostatic repulsion between positive charges. Surface of CNF becomes negatively charged when the pH increases and electrostatic repulsion disappears in the basic medium hence the adsorption quantity was increased.[26,31,32] In the case of PM, adsorption quantity was decreased initially when the pH increases followed by an increase at the basic pHs. The increased adsorption at the acidic pHs is due to cation exchange which becomes more favorable as a result of increased positive charges on CNF surface at pH 1.2. Adsorption quantity is moderate at the pHs around pH_{PZC} of CNF indicating the important contribution of π-π dispersion interactions. Cationic PM molecules are pulled by the negatively charged CNF surface by electrostatic attraction forces which become effective at the alkaline pHs hence the adsorption quantity was found to be higher importantly.[26,33–35]

4 | CONCLUSIONS

Carbon materials are efficient adsorbents for the organic molecules.[36] Carbon based materials such as CNF become prominent expecially for pharmaceutical and biomedical applications for being green and environmentally friendly materials besides their high degree of biocompatibility.[37–42] Adsorption method keeps its advantages such as being economical and easy to handle for the removal of organic and inorganic species from various environments.[43–45] Adsorption capacity of carbon nanofibers (CNF) was tested for two different types of drugs in SGF and SIF. H type Giles isotherms showed the high affinity of drug molecules to CNF surface. Adsorption capacities of CNF were calculated using the Langmuir model as 18.35 and 41.15 mg/g for TMP; and 95.24 and 80.65 mg/g for PM in SGF and SIF, respectively. Results found showed the feasibility of CNF as an alternative commercial gastrointestinal adsorbent. CNF showed moderate adsorption capacity for TMP and high adsorption capacity for PM. Results also enlighten that CNF can be used to remove drugs for other potential applications such as wastewater treatment which is consistent to our previous studies done using CNF.[20] Adsorption kinetics followed the Pseudo second order model for both of the drugs. Plots of intraparticle diffusion demonstrated that PM adsorption has the intraparticle diffusion step as rate controlling step with the boundary layer effect. However, the rate controlling step for TMP adsorption is the diffusion through the boundary layer. Hydrophobic interaction and π-π dispersion interactions played role on the TMP adsorption while cation exchange and electrostatic attraction is important along with the dispersion interactions for PM adsorption.

ACKNOWLEDGMENTS

Betül Berber and Kübra İsanç have contributed to this study equally although second and third author names were ordered alphabetically.

CONFLICT OF INTEREST

The authors confirm that there are no relevant financial or non-financial competing interests to report.

DATA AVAILABILITY STATEMENT

The data that support the findings of this study are available from the corresponding author upon reasonable request.

ORCID

Elif Caliskan Salihi https://orcid.org/0000-0001-7852-3782

REFERENCES

1. Mégarbane B, Oberlin M, Alvarez J-C, et al. Management of pharmaceutical and recreational drug poisoning. *Annals of intensive care*. 2020;10(1):1-30.
2. Otero M, Grande CA, Rodrigues AE. Adsorption of salicylic acid onto polymeric adsorbents and activated charcoal. *React Funct Polym*. 2004;60:203-213.
3. Sah SK, Joshi D, Pathak S, et al. Effect of Ethanol and pH on the In Vitro adsorption of Diazepam onto activated charcoal from simulated gastric fluid and simulated intestinal fluid. *Indian Journal of Pharmaceutical Sciences*. 2017;78(5):624-630.
4. Stefan M, Stefan I, Negoita I-A, Ordeanu V, Stefan DS. Influence of Internal Structure of the Sorbents on Diazepam Sorption from Simulated Intestinal Fluid. *Applied Sciences*. (2021);11(3):1158.
5. Regmi S, Regmi B, Shyaula SL, Pathak S, Bhattarai BP, Sah SK. In vitro study of adsorption kinetics of dextromethorphan syrup onto activated charcoal in simulated gastric and intestinal fluids. *Journal of Chemistry*. 2017;2017.
6. Nabais JMV, Mouquinho A, Galacho C, Carrott PJM, Ribeiro Carrott MML. In vitro adsorption study of fluoxetine in activated carbons and activated carbon fibres. *Fuel Process Technol*. 2008;89(5):549-555.
7. Salihi EC. Adsorption of Metamizole sodium by activated carbon in simulated gastric and intestinal fluids. *Journal of the Turkish Chemical Society, Section A: Chemistry*. 2017;5(1):237-246.
8. Wang M, Safe S, Hearon SE, Phillips TD. Strong adsorption of polychlorinated biphenyls by processed montmorillonite clays: potential applications as toxin enterosorbents during disasters and floods. *Environ Pollut*. 2019;255:113210.
9. Wang G, Xi Y, Lian C, Zhiming S, Shuilin Z. Simultaneous detoxification of polar aflatoxin B1 and weak polar zearalenone from simulated gastrointestinal tract by zwitterionic montmorillonites. *J Hazard Mater*. 2019;364:227-237.
10. Rasheed U, Ul Ain Q, Yaseen M, et al. Modification of bentonite with orange peels extract and its application as mycotoxins' binder in buffered solutions and simulated gastrointestinal fluids. *J Cleaner Prod*. 2020;267:122105.
11. Wang M, Maki CR, Deng Y, Tian Y, Phillips TD. Development of high capacity enterosorbents for aflatoxin B1 and other hazardous chemicals. *Chem Res Toxicol*. 2017;30(9):1694-1701.
12. Wang M, Hearon SE, Phillips TD. Development of enterosorbents that can be added to food and water to reduce toxin exposures during disasters. *Journal of Environmental Science and Health, Part B*. 2019;54(6):514-524.
13. Budnyak TM, Vlasova NN, Golovkova LP, Slabon A, Tertykh VA. Bile acids adsorption by chitoan-fumed silica enterosorbent. *Colloid and Interface Science Communications*. 2019;32:100194.
14. Petik D, Acs N, Bánhidy F, Czeizel AE. A study of the potential teratogenic effect of large doses of promethazine used for a suicide attempt by 32 pregnant women. *Toxicol Ind Health*. 2008;24(1-2):87-96.
15. Nordstrand IAJ Anaphylaxis to trimethoprim: An underappreciated risk in acute medical care. *Emerg Med*. 2004;16(1):82-085.
16. De Jong KP, Geus JW. Carbon nanofibers: catalytic synthesis and applications. *Catalysis Reviews*. 2000;42(4):481-510.
17. Vajtai R, ed. *Springer handbook of nanomaterials*. Springer Science & Business Media, 2013.
18. Hammel E, Tang X, Trampert M, Schmitt T, Mauthner K, Eder A, Pötschke P. Carbon nanofibers for composite applications. *Carbon*. 2004;42(5-6):1153-1158.
19. Yan J, Dong K, Zhang Y, Wang X, Abdulqawy Aboalhassan A, Yu J, Ding B. Multifunctional flexible membranes from sponge-like porous carbon nanofibers with high conductivity. *Nat Commun*. 2019;10(10):1-9.
20. Salihi C, E T, C E. Adsorptive removal of antipsychotic drug by carbon nanofibers in a batch and fixed bed column system, *Part Sci Technol*. 2022;40(7). https://doi.org/10.1080/02726351.2021.2025178
21. Alam MdS, Naqvi AZ. Influence of organic additives on the clouding phenomena of promethazine hydrochloride solutions. *Colloid Polym Sci*. 2007;285(14):1573-1579.
22. Organization WH, The international pharmacopoeia, *World Health Organization*;2006;2. Geneva, (978-9-241-56301-7).
23. Pitarresi G, Pierro P, Giammona G, Iemma F, Muzzalupo R, Picci N. Drug release from α, β-poly (N-2-hydroxyethyl)-dl-aspartamide-based microparticles. *Biomaterials*. 2004;25(18):4333-4343.
24. Windholz M. *The Merck Index*. 10th ed. Merck & Co, 1983, (0-911910-27-1).
25. Salihi EÇ, Mahramanlıoğlu M. Equilibrium and kinetic adsorption of drugs on bentonite: presence of surface active agents effect. *Appl Clay Sci*. 2014;101:381-389.
26. Salihi EÇ, Wang J, Kabacaoğlu G, Kırkulak S, Šiller L. Graphene oxide as a new generation adsorbent for the removal of antibiotics from waters. *Sep Sci Technol*. 2020:1-9.
27. Giles CH, MacEwan TH, Nakhwa SN, Smith D. A system of classification of solution adsorption isotherms, and its use in diagnosis of adsorption mechanisms and in measurement of specific surface areas of solids. *J Chem Soc*. 1960;111:3973-3993.
28. Giles CH, D'Silva AP, Easton IA. A general treatment and classification of the solute adsorption isotherm part. II. Experimental interpretation. *J Colloid Interface Sci*. 1974;47(3):766-778.
29. Langmuir I The adsorption of gases on plane surfaces of glass, mica and platinum. *J Am Chem Soc*. 1918;40(9):1361-1403.
30. Bagheri AR, Ghaedi M. Magnetic metal organic framework for pre-concentration of ampicillin from cow milk samples. *J Pharm Anal*. 2020;10(4):365-375.
31. Salihi EÇ, Gündüz Z, Seza Baştuğ A. Fast retention of isoniazid on organobentonite prepared using green chemistry approach: contribution of the π interactions. *Sep Sci Technol*. 2019;54(16):2695-2705.
32. Carrales-Alvarado DH, Rodríguez-Ramos I, Leyva-Ramos R, Mendoza-Mendoza E, Villela-Martínez DE. Effect of surface area and physical–chemical properties of graphite and graphene-based materials on their adsorption capacity towards metronidazole and trimethoprim antibiotics in aqueous solution. *Chem Eng J*. 2020;402:126155.
33. Seki Y, Yurdakoç K. Equilibrium, kinetics and thermodynamic aspects of promethazine hydrochloride sorption by iron rich smectite. *Colloids Surf A*. 2009;340(1-3):143-148.
34. Salihi EÇ, Talman RYC, Göktürk S. Preparation and characterization of surfactant loaded clays as drug adsorbents. *J Dispersion Sci Technol*. 2021:1-9.
35. Dimpe KM, Nomngongo PN. Application of activated carbon-decorated polyacrylonitrile nanofibers as an adsorbent in

dispersive solid-phase extraction of fluoroquinolones from wastewater. *J Pharm Anal*. 2019;9(2):117-126.

36. Mahramanlioglu M, Bicer I, Misirli T, Caliskan E, Guel S, Misirli C The removal of anionic naphthalene derivatives by the adsorbents produced from used tires. *Fresenius Environ Bull*. 2006;15:1150-1155.
37. Tran PA, Zhang L, Webster TJ. Carbon nanofibers and carbon nanotubes in regenerative medicine. *Adv Drug Deliv Rev*. 2009;61(12):1097-1114.
38. Chan KW, Liao CZ, Wong HM, Yeung KWK, Tjong SC. Preparation of polyetheretherketone composites with nanohydroxyapatite rods and carbon nanofibers having high strength, good biocompatibility and excellent thermal stability. *RSC Adv*. (2016);6(23):19417-19429.
39. Isoaho N, Peltola E, Sainio S, Koskinen J, Laurila T. Pt-grown carbon nanofibers for enzymatic glutamate biosensors and assessment of their biocompatibility. *RSC Adv*. 2018;8(62):35802-35812.
40. Sato Y, Shibata K-i, Kataoka H, et al. Strict preparation and evaluation of water-soluble hat-stacked carbon nanofibers for biomedical application and their high biocompatibility: influence of nanofiber-surface functional groups on cytotoxicity. *Mol Biosyst*. 2005;1(2):142-145.
41. Demirhan K, Bingol Ozakpinar O, Salihi EC. Green and one step modification of graphene oxide using natural substances. *Fullerenes, Nanotubes and Carbon Nanostructures*. 2021;29:716-723.
42. Vila-Donat P, Marín S, Sanchis V, Ramos AJ. A review of the mycotoxin adsorbing agents, with an emphasis on their multi-binding capacity, for animal feed decontamination. *Food Chem Toxicol*. 2018;114:246-259.
43. Mosavi SH, Zare-Dorabei R, Bereyhi M. Rapid and effective ultrasonic-assisted adsorptive removal of congo red onto MOF-5 modified by CuCl2 in ambient conditions: adsorption isotherms and kinetics studies. *ChemistrySelect*. 2021;6(18):4432-4439.
44. Bereyhi M, Zare-Dorabei R, Mosavi SH. Microwave-assisted synthesis of CuCl-MIL-47 and application to adsorptive denitrogenation of model fuel: response surface methodology. *ChemistrySelect*. 2020;5(46):14583-14591.
45. Nazerdeylami S, Zare-Dorabei R. Simultaneous adsorption of Hg2+, Cd2+ and Cu2+ ions from aqueous solution with mesoporous silica/DZ and conditions optimise with experimental design: kinetic and isothermal studies. *Micro & Nano Letters*. 2019;14(8):823-827.

How to cite this article: Salihi EC, Berber B, İsanç K. Kinetic adsorption of drugs using carbon nanofibers in simulated gastric and intestinal fluids. *Int J Chem Kinet*. 2022;1-9. https://doi.org/10.1002/kin.21620